Applied Catalysis A: General 488 (2014) 183–188

Contents lists available at ScienceDirect

Applied Catalysis A: General

journal homepage: www.elsevier.com/locate/apcata

Enhancement of photocatalytic activity for WO_3 by simple NaOH loading

Tetsuya Kako[a,*], Xianguang Meng[a,b], Jinhua Ye[a,b]

[a] Environmental Remediation Materials Unit, National Institute for Materials Science (NIMS), 1-1 Namiki, Tsukuba, Ibaraki 305-0044, Japan
[b] Graduate School of Chemical Science and Engineering, Hokkaido University, Sapporo 060-0814, Japan

ARTICLE INFO

Article history:
Received 30 June 2014
Received in revised form
25 September 2014
Accepted 29 September 2014
Available online 7 October 2014

Keywords:
Solid base
Band structure
H_2O_2
Bottom of conduction band
Electron consumption.

ABSTRACT

We found a simple method for preparation of NaOH-loaded WO_3 with high photocatalytic activity under visible light irradiation. The sample was characterized with XRD, UV–Vis, VB-XPS, and other methods. From the VB-XPS data, the potentials of bottom of conduction band (CB) and top of valence band (VB) for WO_3 were found to be lifted up by NaOH loading. Furthermore, this NaOH-loaded WO_3 exhibited marked photocatalytic activity for 2-propanol decomposition into CO_2 under visible light irradiation. The activity of 5 wt% of NaOH-loaded WO_3 was 120 times higher than that of pure WO_3. Possible reasons for the higher activity of the NaOH-loaded WO_3 are the raising of the potential of CB and suppression of H_2O_2 accumulation. More detailed analyses were conducted using the reaction mechanism and potentials of VB and CB. This stable solid-base-loaded WO_3 maintains its photocatalytic activity for over 3 months.

1. Introduction

Large amounts of harmful organic compounds of many kinds exist in our daily life, and these harmful ones often damage our health. Such harmful organic compounds must be removed from the environment to protect our safe and comfortable life. Photocatalysis is a useful technology for removing them [1,2]. In photocatalysis, harmful organics are decomposed mainly by photogenerated holes. However, if photogenerated electrons are not consumed, these electrons will recombine easily with holes, leading to a decrease in the photocatalytic activity or deactivation of a photocatalyst.

Photocatalysis functioning under visible light irradiation is regarded as a promising technology for the removal of indoor harmful organics because indoor illumination contains large amounts of visible light. At present, the activity of the reported photocatalysts is limited under visible-light irradiation, and novel visible-light-sensitive photocatalysts with higher activity have been expected. Therefore, development of novel photocatalysts has been studied intensively [3–16].

As a binary-oxide semiconductor, WO_3 shows high activity for photocatalytic O_2 evolution from an aqueous $AgNO_3$ solution under visible-light irradiation [17,18]. However, its photocatalytic activity for gaseous organic decomposition is limited [19]. Therefore, investigations of several kinds have been undertaken to enhance its photocatalytic activity [20–23]. Indeed, co-catalyst loading including Pt or Pd is a good method for higher activity [24,25]. However, because Pt and Pd are precious metals, these metals cannot be used in the WO_3 photocatalyst in large amounts. These precious metals probably deactivates easily by catalyst poisoning of sulphur-containing gases such as H_2S and CH_3SH in human living environments [26]. Consequently, in terms of costs, visible-light-sensitive photocatalysts of different types are also needed for varieties of the photocatalysts.

The addition of alkali hydroxide enhances the photocatalytic water-splitting property over Pt-loaded TiO_2- and $SrTiO_3$-related materials [27–30]. This enhancement reportedly suppresses reverse reactions ($2H_2 + O_2 = 2H_2O$) on the Pt surface by alkali addition [27,31]. However, this enhancement mechanism is not always applicable for the case of photocatalytic organic decomposition because the reaction system for water splitting differs greatly from that for organic decomposition. Furthermore, photocatalytic decomposition of gaseous organics in alkali condition has been reported slightly. It should be intensively studied.

Very recently, Aminian and Hakimi partially reported some effects of AOH (A = Na, K, and Cs) on photocatalytic activity for WO_3 [32]. According to his report, 0.075 wt% of KOH-loaded WO_3 showed about four times higher activity than pure WO_3 for gaseous

* Corresponding author. Tel.: +81 29 859 2848; fax: +81 29 860 4958.
E-mail address: kako.tetsuya@nims.go.jp (T. Kako).

http://dx.doi.org/10.1016/j.apcata.2014.09.046
0926-860X/

organic decomposition., However, they also described that too much AOH loading, such as 5 wt% of loading, decreased the activity of WO_3 largely. In addition, Wada et al. described that WO_3 resolves well in the solution with high NaOH concentration, including 1 mol/L of an aqueous NaOH solution, for a short time. Its application is extremely limited because of this dissolution [33].

So, the effect of a large amount of NaOH loading, such as over 5 wt% of loading, on the WO_3 photocatalytic activity and stability remains unclear. More experiments are needed. Therefore, we examined photocatalytic activity of 5 wt% of NaOH-loaded WO_3 under visible-light irradiation in this study. Especially, we carefully prepared 5 wt% of NaOH-loaded WO_3 by controlling the preparation condition including heating temperature. Results show that our prepared NaOH (solid base)-loaded WO_3 showed marked photocatalytic activity and high durability for organics decomposition in the gas phase.

2. Experimental

2.1. Material preparation

Powder of NaOH-loaded WO_3 was prepared by the following method: 10 mL of an aqueous NaOH (Wako Pure Chemical Industries Ltd., Japan) solution (NaOH concentration: 20 g/L) and 4 g of monoclinic WO_3 (Wako) [34] were mixed on a mortar for over 30 min, and the mixed powder was dried in an oven at 343 K for 4–5 h. Finally, we obtained the sample, of which the mixing ratio of NaOH to WO_3 was 5 wt% (NaOH: WO_3 = 5:100). Additionally, 25 wt% of NaOH-loaded WO_3 was prepared by using this method. As a reference sample, 0.075 wt% of KOH-loaded WO_3 powder was prepared using the method described in the earlier report. This powder was obtained by heating of the mixed KOH-WO_3 powder at 723 K for 2 h [32].

2.2. Material characterization

The prepared samples were first characterized with an X-ray diffraction meter (XRD, X'pert Pro; PANalytical Co., Netherlands) with Cu Kα radiation. Using the Kubelka–Munk relationship, optical absorption spectra of the prepared samples were converted from their respective reflectance spectra, which were measured using a UV–Vis spectrophotometer (UV-2500PC; Shimadzu Corp. Japan).

Results of valence-band X-ray photoemission spectroscopic data (VB-XPS) were obtained by measuring the samples using an X-ray photoelectron spectrometer (AXIS-HS; Shimadzu-Kratos Analytical Com., Japan) with an X-ray source of monochromatic Al. Binding energy was calibrated using C 1s peak with binding energy of 284.5 eV.

Photocatalytic activity at room temperature was evaluated from 2-propanol (IPA) into CO_2 via acetone. Details of the evaluation method are the following: the powder sample with weight of 0.4 g spread evenly on the dish with the area of about 8 cm^2. The dish was set on the glass reactor with a volume of 500 cm^3. The inside atmosphere of the reactor was replaced with pure air. Furthermore, IPA gas was injected into the reactor. Then, the concentration of the IPA in the reactor was estimated as 700–800 ppm. Subsequently, the reactor was kept in the dark until the IPA gas reached the adsorption–desorption equilibrium state. Then, the reactor was irradiated with visible light (400 nm < λ < 530 nm), which was emitted from a 300-W Xe lamp equipped with a water filter and glass filters of three kinds [UV-cutoff filter (Y-44), blue filter (B390), and IR cutoff filter (HA-30), Hoya. Corp., Japan]. The light intensity was about 1 mW cm^{-2}, which was evaluated using a spectroradiometer (UV-40, Ushio Inc., Japan). The IPA, acetone, and CO_2 gases were measured using a gas chromatograph (GC-14B; Shimadzu) with flame-ionized detectors (FID) and a methanizer.

The specific surface area was evaluated with a surface area analyzer (Gemini-2460; Micromeritics Instrument Corp., USA) using Brunauer-Emmett-Teller (BET) method at 77 K. Furthermore, the areas were 5.8, 7.0, 8.6, and 4.5 m^2/g, respectively, for pure WO_3, 5 wt%-NaOH-WO_3, 25 wt%-NaOH-WO_3, and 0.075 wt%-KOH-WO_3.

3. Results and discussion

3.1. XRD

Fig. 1 presents the XRD patterns of pure WO_3 and 5 wt% of NaOH-loaded WO_3. From the XRD results and data from an earlier report [34], the 5 wt% of NaOH-loaded WO_3 mainly consists of monoclinic WO_3 (PDF No. 43-1035). A small amount of crystallized $Na_2WO_4{\cdot}2H_2O$ with orthorhombic structure (PDF No. 13-0431) also exists in the sample. Reportedly, WO_3 can partially react with NaOH. Thereby, $Na_2WO_4{\cdot}2H_2O$ can be formed [35].

3.2. Optical absorption property

As described above, the new phase was formed on the sample (NaOH-loaded WO_3) and this formation might affect the absorption property. Therefore, optical absorption spectra were measured using a UV–vis spectrophotometer. We checked an effect of the NaOH loading on the optical absorption property. Fig. 2 presents the optical absorption spectra of WO_3 and the 5 wt% of NaOH-loaded WO_3. Both samples can absorb visible light well. Furthermore,

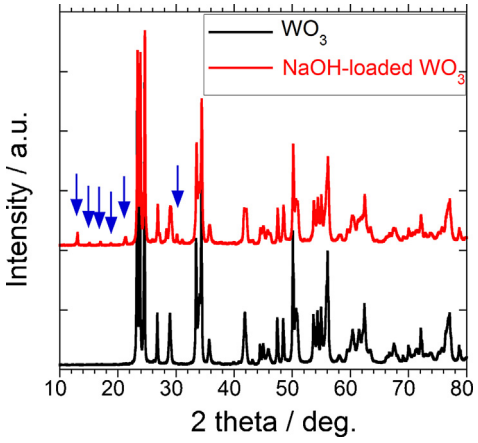

Fig. 1. XRD patterns of pure WO_3 and 5 wt% of NaOH-loaded WO_3. Arrows indicate the XRD patterns of $Na_2WO_4{\cdot}2H_2O$.

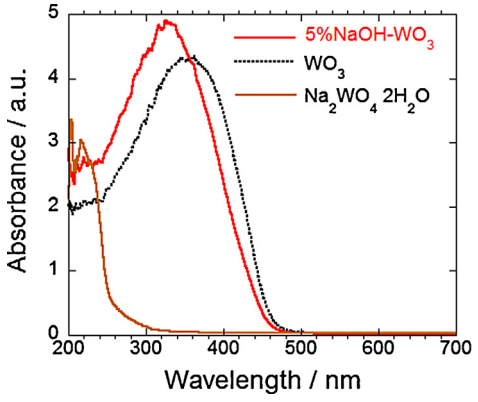

Fig. 2. Optical absorption spectra of WO_3 and 5 wt% of NaOH-loaded WO_3.

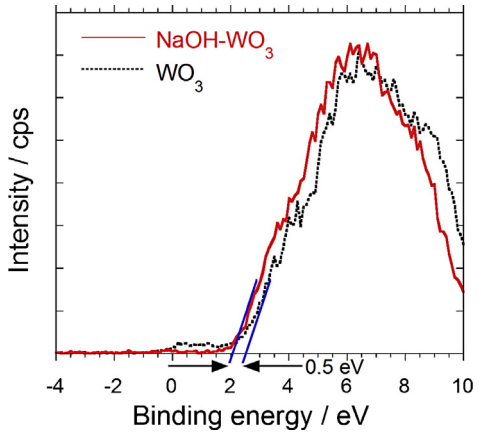

Fig. 3. VB-XPS spectra of WO_3 and 5 wt% of NaOH-loaded WO_3.

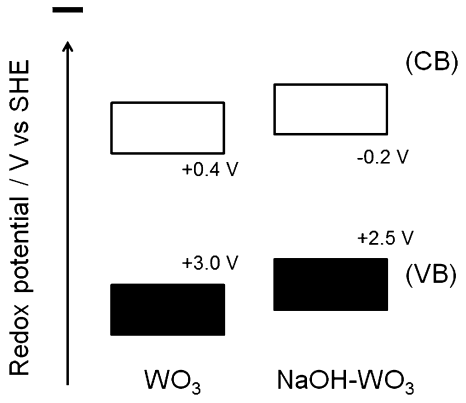

Fig. 4. Schematic illustration of proposed band structure of WO_3 and 5 wt% of NaOH-loaded WO_3.

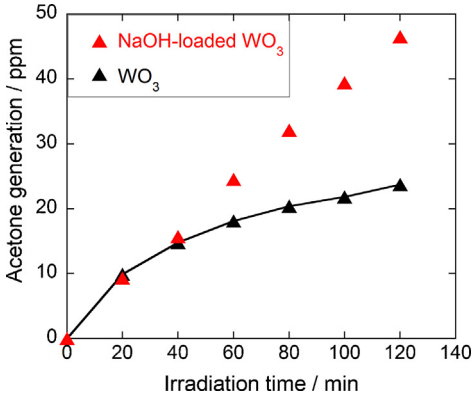

Fig. 5. Photocatalytic IPA decomposition into acetone at the initial stage under visible-light irradiation over WO_3 and 5 wt% of NaOH-loaded WO_3.

results show that the absorption spectrum of the NaOH-loaded WO_3 slightly blue-shifted compared with that of WO_3. This blue shift is possibly attributable to the change in surface functional groups [36,37] and existence of other compounds including NaOH with white colour.

Next, the absorption properties were evaluated qualitatively to elucidate their differences in the properties. First, the band gaps were calculated from the onset absorption edges [38]. The band gaps of pure WO_3 and the NaOH-loaded WO_3 were estimated, respectively, as 2.6 and 2.7 eV. As a reference, the absorption spectrum of $Na_2WO_4{\cdot}2H_2O$ was also measured and the band gap was about 4.1 eV. Its band gap is over 1 eV larger than that of the NaOH-WO_3, so formation of Na_2WO_4 does not affect the VB-XPS data (described in Section 3.3) around the top of VB for the NaOH-WO_3.

3.3. Band structure

The band structure of a photocatalyst usually affects its photocatalytic activity. Therefore, information related to the band structure is important. Consequently, the potentials for top of the valence band (VB) for the samples were estimated. Then, the band structures were discussed using these estimated potentials and the band gaps.

First, the potentials for top of the VB were estimated using VB-XPS technique. Fig. 3 presents the XPS spectra of the samples at around 0 eV in the binding energy. This result suggests that the potential for the top of VB for the NaOH-loaded WO_3 was 0.5 eV smaller than that for WO_3. Furthermore, the potential for top of VB for WO_3 can be estimated as +3.0 V (vs SHE) because the potential for bottom of CB was reported as +0.4 V (vs SHE) [39] and its band gap was 2.6 eV. Therefore, the potentials for the top of VB and bottom of CB for the NaOH-loaded WO_3 were estimated as –0.2 and +2.5 V (vs SHE), respectively. Based on these results, the band structure can be written as shown in Fig. 4.

The reason why the potential for top of VB is less positive by NaOH loading remains unclear, but a possible reason is the following. The potential of top of VB has been reported as less positive in an alkali solution. This shift obeys the relation presented in Eq. (1).

$$V^0 = V^0(\mathrm{pH}\,0) - 0.06\mathrm{pH} \quad (1)$$

Here V^0 denotes the potential of the top of VB [40]. This relation might be extended to solid-base-loaded semiconductor (photocatalyst). For 5 wt%-NaOH-WO_3, the surface is basic. When the sample was prepared, an aqueous NaOH solution (pH >13) was used. For pure WO_3, the surface is neutral. It is surrounded with air and adsorbed water (pH ≈ 7). If the shift above (Eq. (1)) occurs in this system, then the potential of the top of VB of 5 wt%-NaOH-WO_3 would be at least 0.4 V lower than that of pure WO_3. This value is close to that of the shift (0.5 eV), which was measured by VB-XPS. Therefore, we consider that this kind of the shift may occur on the base (NaOH)-coated photocatalyst surface.

3.4. Photocatalytic activity

Photocatalytic activity was evaluated from IPA decomposition into CO_2 via acetone because IPA is a frequently used VOC in industry. In addition, the IPA decomposition is a standard reaction for photocatalytic-activity evaluation [11,15]. First, we evaluated IPA decomposition into acetone by photogenerated holes at the initial reaction stage. Fig. 5 shows a change in concentrations of acetone generation in IPA decomposition between 0 and 2 h of visible-light irradiation. Between 0 and 40 min, the acetone concentration over WO_3 is almost equal to that over the NaOH-loaded WO_3. Subsequently, however, pure WO_3 was partially deactivated. The acetone concentration for WO_3 is half that for the NaOH-loaded WO_3 at 2 h of light irradiation. This result suggests that the NaOH loading does not work as enhancement of WO_3 photocatalytic activity itself. However, the loading functions as suppression of deactivation for WO_3 activity. By further visible light irradiation, intermediate acetone can be decomposed into the final product CO_2 by photogenerated holes. Results show more marked difference in the activity between WO_3 and the NaOH-loaded WO_3, as shown in Fig. 6. The figure shows the time dependence of changes of acetone and CO_2 concentrations over WO_3 and the NaOH (5 wt%)-loaded WO_3. For the NaOH-loaded WO_3, acetone was generated mainly. The concentration of acetone generation increased linearly with irradiation time of 0–24 h. After about 24 h, the concentration of acetone in the

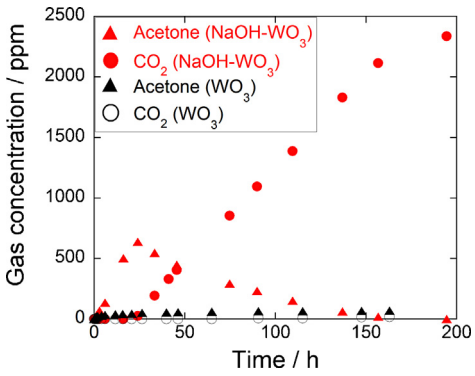

Fig. 6. Photocatalytic IPA decomposition into CO_2 via acetone between 0 and 200 h under visible-light irradiation over WO_3 and 5 wt% of NaOH-loaded WO_3.

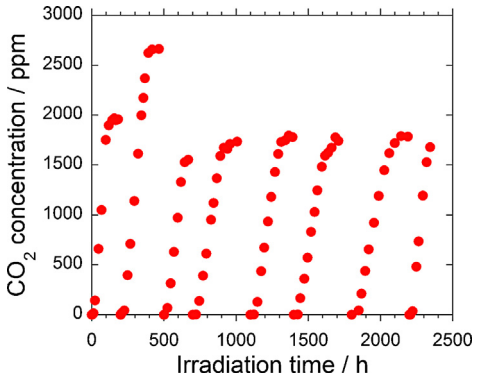

Fig. 7. Repeated tests for photocatalytic decomposition of IPA into CO_2 over 25 wt% of NaOH-loaded WO_3 under visible-light irradiation. 600–800 ppm of IPA gas in every turn except for the second run was injected into the reactor. In the second run, 860 ppm of IPA was injected.

gas phase decreased and CO_2 concentration increased drastically and linearly, indicating that intermediate acetone was decomposed into CO_2. Furthermore, after about 200 h of visible-light irradiation, the injected IPA was decomposed almost completely into CO_2 by photogenerated holes for the NaOH-loaded WO_3. For WO_3, the concentrations of acetone and CO_2 generation increased slowly with irradiation time. The concentrations were extremely low. When the photocatalytic activity of the NaOH-loaded WO_3 is compared with that of pure WO_3 using CO_2 concentrations after 160 h, the activity of the NaOH (5 wt%)-loaded WO_3 was over 120 times higher than that of pure WO_3. Larger surface area contributed little to higher photocatalytic activity of 5 wt%-NaOH-WO_3 because the surface area of the 5 wt%-NaOH-WO_3 (7.0 m^2/g) was only 1.2 times higher than that of pure WO_3 (5.8 m^2/g). The reason for this higher surface area is expected to derive from NaOH coverage of the 5 wt%-NaOH-WO_3 surface.

The NaOH-loaded WO_3 shows much higher activity than WO_3, which might be attributable to the ease of consumption for photogenerated electrons. Apparently, the reactions for consumption of photogenerated electrons on the NaOH-loaded WO_3 should be different from those for WO_3. For WO_3, photogenerated electrons can be reacted with O_2 through two-electron oxygen reduction (Eq. (4)), and H_2O_2 is formed [41]. However, H_2O_2 is saturated quickly and the rate for H_2O_2 consumption is very slow (ESI, Fig. S1) [41], indicating that H_2O_2 formation almost stops on the WO_3 after saturation. Because the other electron consumption cannot occur, little electron consumption occurs at H_2O_2 saturation. Therefore, the photogenerated electrons are accumulated on the WO_3. The electrons recombine easily with holes, thereby greatly decreasing the activity quickly.

For the NaOH-loaded WO_3, the electrons can be consumed by one-electron or two-electron O_2 reductions. These reduction reactions engender ease of consumption for photogenerated electrons, as described below. As shown in Fig. 4, the potential for the bottom of CB for the NaOH-loaded WO_3 is more negative than potentials for one-electron O_2 reduction (Eqs. (2) and (3)) [24]. Therefore, one-electron O_2 reduction may occur. The rate of this reduction is regarded as much higher than that of the two-electron oxygen reduction (Eq. (4)) or H_2O_2 consumption reaction [42], leading to higher activity of the NaOH-loaded WO_3. To elucidate this proposed mechanism, we will plan to systematically investigate the formation of $\cdot O_2^-$ or $\cdot$OOH radical by ESR or other technique. We will discuss it in a future report.

Aside from one-electron O_2 reduction, two-electron O_2 reduction (Eqs. (4) and (6)) is expected to occur on the NaOH-loaded WO_3. For the reduction described in Eq. (4), one must consider whether H_2O_2 is saturated on the surface of the NaOH-loaded WO_3. This is because H_2O_2 saturation decreases the photocatalytic activity easily and heavily, just as WO_3. However, under alkaline environment, H_2O_2 becomes more reactive [43]. It is rapidly decomposed into reactive OOH^- (Eq. (5)), which further reacts with the photoexcited electrons (Eq. (6)). Therefore, for NaOH-loaded WO_3, H_2O_2 can be consumed more easily via Eqs. (5)–(7) [44]. The rate of consumption of H_2O_2 for NaOH-loaded WO_3 is expected to be much higher than that for pure WO_3, leading to higher activity of NaOH-loaded WO_3. This expectation is supported by measurement of the H_2O_2 amount on the photocatalyst surface; the amount of H_2O_2 on the NaOH-WO_3 was much smaller than that on pure WO_3 (ESI, Fig. S3).

$$O_2 + H^+ + e^- = \cdot OOH\,(-0.046\,V\ vs\ SHE) \quad (2)$$

$$O_2 + e^- = \cdot O_2^-\,(-0.28\,V\ vs\ SHE) \quad (3)$$

$$O_2 + 2H^+ + 2e^- = H_2O_2\ (+0.68\,V\ vs\ SHE) \quad (4)$$

$$H_2O_2 = H^+ + OOH^- \quad (5)$$

$$OOH^- + H_2O + 2e^- = 3OH^-\,(+0.87\,V\ vs\ SHE) \quad (6)$$

$$2OOH^- = O_2 + 2OH^- \quad (7)$$

$$H^+ + OH^- = H_2O \quad (8)$$

As described above, the 5 wt% of NaOH-loaded WO_3 showed relatively high activity. Furthermore, a larger amount of NaOH-loaded sample, 25 wt% of NaOH-loaded WO_3 showed visible-light sensitivity (ESI, Fig. S2) and relatively high activity. Its activity resembles the activity of 5 wt% of NaOH-loaded WO_3. In addition, 25 wt% of NaOH-loaded WO_3 consisting of WO_3, Na_2WO_4, and NaOH (ESI, Figs. S3 and S4) shows stable photocatalytic performance for a long time, as shown in Fig. 7. The figure shows repeated tests for CO_2 generation in photocatalytic IPA decomposition under visible-light irradiation over 25 wt% of NaOH-loaded WO_3. Based on this result, we found that the photocatalyst maintains its relatively high activity for about 3 months. Furthermore, if 1 mol of IPA (C_3H_8O) is considered to be decomposed into 3 mol of CO_2 by 18 holes [45,46], just as Eq. (9), the turnover number (TON) of this photocatalyst became about 1.1 after the eighth run of the photocatalytic repeated tests. Therefore, we conclude that the IPA decomposition over the NaOH-loaded WO_3 should be regarded as a genuine photocatalytic reaction.

$$C_3H_8O + 5H_2O + 18h^+ = 3CO_2 + 18H^+ \quad (9)$$

The results of the activity and heating temperature reported herein completely differ from those of previously reported study by Aminian et al. [32]. In that study, 5 wt% of alkali loading at 723 K was too large. In addition, loading of too much alkali hydroxide cannot enhance the photocatalytic activity of WO_3 because of the complete phase transition and morphology changes from nanoparticles into nanorods. Furthermore, 0.075 wt% of KOH-loaded WO_3

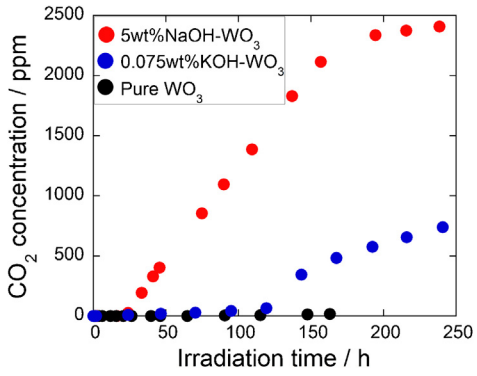

Fig. 8. Photocatalytic IPA decomposition into CO_2 under visible-light irradiation over WO_3, 5 wt% of NaOH-loaded WO_3, and 0.075 wt% of KOH-loaded WO_3.

prepared at 723 K reportedly showed the highest activity among the KOH-loaded WO_3 samples, with loading amounts of 0–5 wt% reported for their study. Therefore, we prepared 0.075 wt% of KOH-loaded WO_3 as a reference sample and compared its photocatalytic activity with the activity of our 5 wt% of NaOH-loaded WO_3 to elucidate the activity difference between this study and the previously reported studies. Fig. 8 shows the time dependence of change of CO_2 generation in IPA decomposition under visible-light irradiation in the presence of some photocatalysts. Indeed, IPA can be decomposed by photocatalysis of 0.075 wt% of KOH-loaded WO_3. However, the activity for the 0.075 wt% of KOH-loaded WO_3 was over four times lower than that for the 5 wt% of NaOH-loaded WO_3 when the activity was evaluated from concentrations of CO_2 generation after about 160 h of light irradiation. The higher activity of the 5 wt%-NaOH-loaded WO_3 was first considered. Since the morphology changes were reported to lead to decrease in the activity as described above [32], the morphology of pure WO_3 and these two alkali-treated WO_3 was measured using SEM, which revealed no marked difference (ESI, Fig. S4). These three samples were composed entirely of nanoparticles, indicating that morphology changes that led to decreased activity did not occur by 5 wt%-NaOH-loading at 343 K. Namely, results show that 5 wt%-NaOH-loading at low temperature did not change the morphology. In addition, because a larger amount of alkali loading can promote electron consumption as described above, the 5 wt%-NaOH-loaded WO_3 can show higher activity than the 0.075 wt%-KOH-loaded WO_3. Aside from these factors, the larger surface area contributed slightly to higher activity of the 5 wt%-NaOH-loaded WO_3. The activity for the 0.075 wt% of KOH-loaded WO_3 annealed at 723 K was reportedly much higher than that for 5 wt% of KOH-loaded WO_3 at 723 K. Therefore, it can be inferred that 5 wt% of NaOH-loaded WO_3 heated at 343 K shows much higher activity than 5 wt% of KOH-loaded WO_3 at 723 K with phase-transferred nanorods. From these results, we infer that the heating temperature is also an important factor for higher activity. Furthermore, we concluded that an amount of NaOH loaded should be large (5–25 wt%). The loaded sample should be dried at low temperature, such as 343 K and room temperature, for development of NaOH-loaded WO_3 with higher activity.

4. Conclusion

We developed 5 wt% of NaOH-loaded WO_3 sample, which was prepared by drying the mixture of NaOH and WO_3 at 343 K. This sample showed marked photocatalytic activity for 2-propanol decomposition into CO_2 under visible light irradiation. The activity of this sample was 120 times higher than that of pure WO_3. This higher activity might derive from ease of photogenerated electrons for the NaOH-loaded WO_3, judging from the initial stage of 2-propanol decomposition and stable photocatalytic performance of the NaOH-loaded WO_3.

IPA is mainly decomposed by photogenerated holes. However, if photogenerated electrons do not consume well, then recombination between holes and electrons occurs easily, leading to deactivation or low activity of the photocatalyst. Therefore, consumption of electrons is extremely important. For pure WO_3, electrons are first consumed through two-electron O_2 reduction and H_2O_2 forms. However, H_2O_2 cannot be decomposed well and saturated on the surface, leading to decrease in the activity. However, for NaOH-loaded WO_3, electrons can be consumed by two reactions including one-electron and two-electron O_2 reduction. For two-electron O_2 reduction, H_2O_2 may form, but this H_2O_2 is decomposed more easily because H_2O_2 becomes reactive in alkali conditions. For one-electron O_2 reduction, H_2O_2 does not form and accumulate on the surface, leading to maintenance of its activity.

Additionally, results show that the activity of NaOH (solid base)-loaded WO_3 is affected strongly by heating temperature and loading amount of NaOH. Low heating temperature and a large loading amount engender higher photocatalytic activity. Results show that the 5 wt% of NaOH-loaded WO_3 heated at 343 K for this study showed over four times higher activity than the 0.075 wt% of KOH-loaded WO_3 described in the earlier report. In addition, 25 wt% of NaOH-loaded WO_3 shows relatively high photocatalytic activity and retains its photocatalytic activity for about 3 months. Based on these results, we conclude that solid-base loading is a promising method for the development of stable photocatalysts with high activity.

Appendix A. Supplementary data

Supplementary data associated with this article can be found, in the online version, at http://dx.doi.org/10.1016/j.apcata.2014.09.046.

References

[1] M.R. Hoffmann, S.T. Martin, W.Y. Choi, D.W. Bahnemann, Chem. Rev. 95 (1995) 69–96.
[2] K. Hashimoto, H. Irie, A. Fujishima, Jpn. J. Appl. Phys. 44 (2005) 8269–8285.
[3] M. Liu, X. Qiu, M. Miyauchi, K. Hashimoto, J. Am. Chem. Soc. 135 (2013) 10064–10072.
[4] T. Kako, J. Ye, J. Mol. Catal. A 320 (2010) 79–84.
[5] H.G. Kim, D.W. Hwang, J.S. Lee, J. Am. Chem. Soc. 126 (2004) 8912–8913.
[6] A. Tanaka, K. Hashimoto, H. Kominami, J. Am. Chem. Soc. 134 (2012) 14526–14533.
[7] N. Murakami, T. Matsuo, T. Ohno, Catal. Commun. 12 (2011) 341–344.
[8] H. Irie, S. Miura, K. Kamiya, K. Hashimoto, Chem. Phys. Lett. 457 (2008) 202–205.
[9] J.Z. Bloh, R. Dillert, D.W. Bahnemann, Environ. Sci. Pollution Res. 19 (2012) 3688–3695.
[10] Z.G. Yi, J.H. Ye, N. Kikugawa, T. Kako, S.X. Ouyang, H. Stuart-Williams, H. Yang, J.Y. Cao, W.J. Luo, Z.S. Li, Nat. Mater. 9 (2010) 559–564.
[11] R. Asahi, T. Morikawa, T. Ohwaki, K. Aoki, Y. Taga, Science 293 (2001) 269–271.
[12] T. Kako, N. Umezawa, K. Xie, J. Ye, J. Mater. Sci. 48 (2013) 108–114.
[13] S.U.M. Khan, M. Al-Shahry, W.B. Ingler, Science 297 (2002) 2243–2245.
[14] D.F. Wang, T. Kako, J. Ye, J. Am. Chem. Soc. 130 (2008) 2724–2725.
[15] T. Kako, Z.G. Zou, M. Katagiri, J.H. Ye, Chem. Mater. 19 (2007) 198–202.
[16] W. Macyk, G. Burgeth, H. Kisch, Photochem. Photobiol. Sci. 2 (2003) 322–328.
[17] T. Kako, N. Kikugawa, J.H. Ye, Catal. Today 131 (2008) 197–202.
[18] A. Kudo, K. Ueda, H. Kato, I. Mikami, Catal. Lett. 53 (1998) 229–230.
[19] T. Arai, M. Yanagida, Y. Konishi, Y. Iwasaki, H. Sugihara, K. Sayama, Catal. Commun. 9 (2008) 1254–1258.
[20] K. Katsumata, R. Motoyoshi, N. Matsushita, K. Okada, J. Hazardous Mater. 260 (2013) 475–482.
[21] L. Huang, H. Xu, Y. Li, H. Li, X. Cheng, J. Xia, Y. Xu, G. Cai, Dalton Trans. 42 (2013) 8606–8616.
[22] A.J.E. Rettie, K.C. Klavetter, J.F. Lin, A. Dolocan, H. Celio, A. Ishiewkene, H.L. Bolton, K.N. Pearson, N.T. Hahn, C.B. Mullins, Chem. Mater. 26 (2014) 1670–1677.
[23] C.W. Dunnill, S. Noimark, I.P. Parkin, Thin Solid Films 520 (2012) 5516–5520.
[24] R. Abe, H. Takami, N. Murakami, B. Ohtani, J. Am. Chem. Soc. 130 (2008) 7780–7781.
[25] T. Arai, M. Horiguchi, M. Yanagida, T. Gunji, H. Sugihara, K. Sayama, Chem. Commun. (2008) 5565–5567.

[26] T. Kako, H. Irie, K. Hashimoto, J. Photochem. Photobiol. A 171 (2005) 131–135.
[27] S. Sato, J.M. White, J. Catal. 69 (1981) 128–139.
[28] S.X. Ouyang, H. Tong, N. Umezawa, J. Cao, P. Li, Y. Bi, Y. Zhang, J. Ye, J. Am. Chem. Soc. 134 (2012) 1974–1977.
[29] K. Domen, S. Naito, T. Onishi, K. Tamaru, Chem. Phys. Lett. 92 (1982) 433–434.
[30] F.T. Wagner, G.A. Somorjai, Nature 285 (1980) 559–560.
[31] M. Kitano, M. Hara, J. Mater. Chem. 20 (2010) 627–641.
[32] M.K. Aminian, M. Hakimi, Catal. Sci. Technol. 4 (2014) 657–664.
[33] M. Wada, N. Wang, Y. Konishi, Y. Miseki, T. Gunji, K. Sayama, Chem. Lett. 42 (2013) 395–397.
[34] C. Zhao, Y. Yang, Z. Zhang, Open. J. Appl. Sci. 2 (2012) 86–92.
[35] Z. Mirski, T. Piwowarczyk, Arch. Civ. Mech. Eng. 11 (2011) 411–419.
[36] G. Li, T. Kako, J. Ye, J. Phys. Chem. Solid 69 (2008) 2487–2491.
[37] Z. Li, T. Yu, Z. Zou, J. Ye, Appl. Phys. Lett. 88 (2006) 071917.
[38] A. Ishikawa, T. Takata, T. Matsumura, J.N. Kondo, M. Hara, H. Kobayashi, K. Domen, J. Phys. Chem. B 108 (2004) 2637–2642.
[39] S.J. Hong, S. Lee, J.S. Jang, J.S. Lee, Energy Environ. Sci. 4 (2011) 1781–1787.
[40] M.A. Alpuche-Aviles, Y. Wu, J. Am. Chem. Soc. 131 (2009) 3216–3224.
[41] J. Kim, C. Lee, W. Choi, Environ. Sci. Technol. 44 (2010) 6849–6854.
[42] O. Tomita, R. Abe, B. Ohtani, Chem. Lett. 40 (2011) 1405–1407.
[43] A.G. Leigh, US Patent 4,304,762A (1981).
[44] E. Yeager, J. Mol. Catal. 38 (1986) 5–25.
[45] H. Irie, Y. Watanabe, K. Hashimoto, J. Phys. Chem. B 107 (2003) 5483–5486.
[46] H. Shi, G.Q. Chen, Z.G. Zou, Appl. Catal. B 156–157 (2014) 378–384.